

# Fast incorporation of primary amine group into polylactide surface for improving C<sub>2</sub>C<sub>12</sub> cell proliferation using nitrogen-based atmospheric-pressure plasma jets

Yi-Wei Yang,<sup>1</sup> Jane-Yii Wu,<sup>2</sup> Chih-Tung Liu,<sup>1</sup> Guo-Chun Liao,<sup>1</sup> Hsuan-Yu Huang,<sup>1</sup> Ray-Quen Hsu,<sup>1</sup> Ming-Hung Chiang,<sup>1</sup> Jong-Shinn Wu<sup>1</sup>

<sup>1</sup>Department of Mechanical Engineering, National Chiao Tung University, Hsinchu, Taiwan

<sup>2</sup>Department of Bioindustry Technology, Da Yeh University, Changhua, Taiwan

Received 10 December 2012; revised 3 February 2013; accepted 5 February 2013

Published online 24 April 2013 in Wiley Online Library (wileyonlinelibrary.com). DOI: 10.1002/jbm.a.34681

**Abstract:** In this article, we report the development of the fast incorporation of primary amine functional groups into a polylactide (PLA) surface using the post-discharge jet region of an atmospheric-pressure nitrogen-based dielectric barrier discharge (DBD). Plasma treatments were carried out in two sequential steps: (1) nitrogen with 0.1% oxygen addition, and (2) nitrogen with 5% ammonia addition. The analyses show that the concentration of N/C ratio, surface energy, contact angle, and surface roughness of the treated PLA surface can reach 19.1%, 70.5 mJ/m<sup>2</sup>, 38° and 73.22 nm, respectively. In addition, the proposed two-step plasma treatment

procedure can produce a PLA surface exhibiting almost the same C<sub>2</sub>C<sub>12</sub> cell attachment and proliferation performance as that of the conventional gelatin coating method. Most importantly, the processing/preparation time is reduced from 13–15 h (gelatin coating method) to 5–15 min (two-step plasma treatment), which is very useful in practical applications. © 2013 Wiley Periodicals, Inc. *J Biomed Mater Res Part A*: 102A: 160–169, 2014.

**Key Words:** atmospheric-pressure, plasma, DBD, tissue engineering, biomaterial, PLA, cell proliferation

**How to cite this article:** Yang Y-W, Wu J-Y, Liu C-T, Liao G-C, Huang H-Y, Hsu R-Q, Chiang M-H, Wu J-S. 2014. Fast incorporation of primary amine group into polylactide surface for improving C<sub>2</sub>C<sub>12</sub> cell proliferation using nitrogen-based atmospheric-pressure plasma jets. *J Biomed Mater Res Part A* 2014;102A:160–169.

## INTRODUCTION

One of the challenges in tissue engineering, especially in cases requiring immediate implant operation, is to proliferate the cells obtained from a patient using *in vitro* cell culture to an acceptable number of cells in a short period of time and transplant them into a 3D scaffold, which would be subsequently implanted in the patient.<sup>1,2</sup> In addition, shortening the preparation time of culture substrates is another crucial challenge in these cases. However, the culture substrates are usually made of polymers. As a result, they often have a low surface energy, hydrophobic features and a lack of natural binding sites for cells, which greatly hinders cell attachment on their surfaces.<sup>3</sup> As an example, polylactide (PLA) is increasingly being used as either a cell culture substrate or an implant scaffold due to its good mechanical properties, non-cytotoxicity, and degradability.<sup>4</sup> However, PLA suffers from the same problems (such as low cell attachment) as most polymer materials. Thus, the questions of how to improve cell attachment, speed up cell proliferation but also reduce the preparation time of culture substrates are important for better tissue engineering.

Quality of cell attachment significantly influences subsequent cell proliferation.<sup>5</sup> Cell attachment is the first phase of cell–material interaction. It is initialized with an adhesive protein layer, which serves to provide binding sites between cells and the material surface. For instance, extra cellular matrix (ECM) proteins, such as fibrinogen, vitronectin, fibronectin, and collagen, as well as peptides with an arginine–glycine–aspartate (RGD) sequence are all effective cell binding sites for cell attachment.<sup>6</sup> With such materials, cells attach to the surface via receptor–ligand interactions. For example, integrins on the cell membrane can interact with a representative glycoprotein in the ECM (fibronectin) that contains a ligand for binding integrin receptors, allowing the formation of focal adhesions.<sup>7</sup> Through receptor–ligand interactions, cells can receive signals to attach and proliferate on the substrate surface. Thus, immobilization of proteins or ligands on the surface of the substrate material is an effective way to activate and improve cell attachment.

To enhance cell attachment and subsequent proliferation on PLA, suitable surface modification is required. In addition, the initial interaction between the material and cells is critical for later development. This interaction is greatly

**Correspondence to:** J.-S. Wu; e-mail: chongsin@faculty.nctu.edu.tw

Contract grant sponsor: National Science of Council of Taiwan; contract grant number: NSC-101-2221-E-009-041-MY3

influenced by chemical and physical properties of the surface, including surface energy, wettability, surface roughness, and the availability of functional groups.<sup>8,9</sup>

The gelatin coating method is one of the widely used approaches to promote cell attachment. Gelatin is a mixture of peptides and hydrolyzed collagen, which is particularly rich in proline and hydroxyproline.<sup>10</sup> In addition, gelatin contains a high concentration of amino acids, such as glycine and arginine. Thus, coated gelatin possesses abundant cell binding sites and also exhibits non-toxic, hydrophilic, and bio-natural characteristics. In other words, it is originally biocompatible and beneficial to cell attachment. However, gelatin coating is a very time-consuming procedure, which generally takes 13–15 h, if not longer.<sup>11,12</sup> Such a lengthy preparation time contradicts the immediate implant requirement mentioned earlier.

Recently, low-temperature plasma treatment has been considered as a promising approach to fulfill both requirements (speed and attachment) as mentioned above. This approach has been applied to polymers, which cannot resist high temperatures, to modify the surface characteristics without altering the bulk material properties. The capabilities of this treatment, including the incorporation of functional groups, enhancement of surface energy, tailoring surface roughness, and increasing wettability, have been demonstrated and widely studied.<sup>13,14</sup> It was shown that low-temperature plasma can be efficiently used to promote cell attachment, due to the fact that amino functional groups can covalently couple with biological ligands to provide receptor–ligand interactions.<sup>15,16</sup> However, most of these implementations operated in low-pressure environments, which are often costly and inconvenient in practice.

Recently, low-temperature atmospheric-pressure plasma (APP) has attracted great attention. Its advantages include the following: (1) low cost because expensive vacuum equipment is not needed and (2) convenient and efficient operation under atmospheric conditions. However, it was found that only a low quantity of amino functional groups could be incorporated using APP<sup>17,18</sup>; this limitation may hinder its further application in related fields.

In this study, we propose a two-step APP treatment procedure to enhance the incorporation of amino functional groups onto the PLA surface, which can enhance cell attachment and proliferation with a significantly reduced preparation time. Surface properties with and without plasma treatments were characterized by contact angle, XPS, ATR-FTIR, and AFM measurements. Biological tests for assessing cell morphology, attachment, and proliferation were performed by cell culture, inverted contrasting microscope observation, and MTT assays, respectively. Various PLAs were used: pure, pretreatment plasma treated, ammonia plasma treated, two-step plasma treated, and gelatin coated. C<sub>2</sub>C<sub>12</sub> mouse muscle myoblast cells were used as the test cells throughout the study.

## METHODS

### Sample preparation

The test polylactic acid (PLA) films were fabricated by a film casting method. The PLA pellets (PLLA/PDLA/95:5,  $M_w$ :

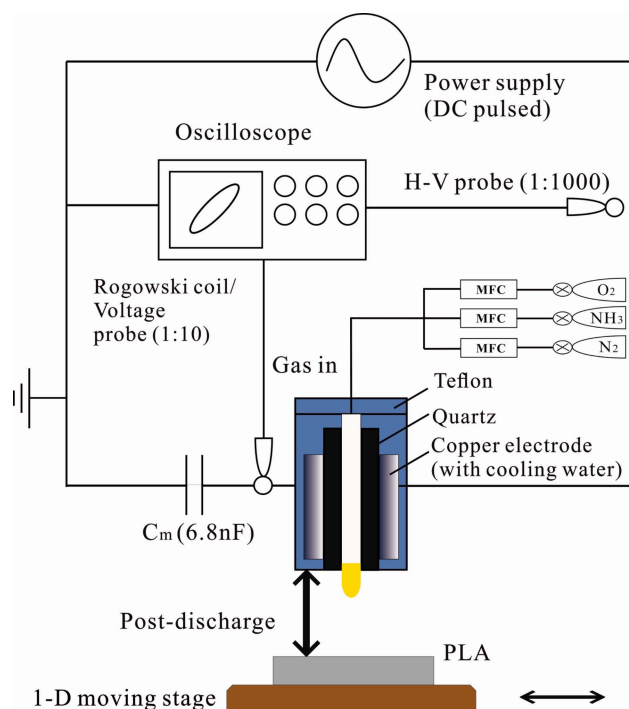


**FIGURE 1.** Schematic diagram of the atmospheric-pressure treatment system. [Color figure can be viewed in the online issue, which is available at [wileyonlinelibrary.com](http://wileyonlinelibrary.com).]

180K ~200K, Wei Mon Industry, Taiwan) were dissolved in chloroform (C-0385, Katayal Chemical, Taiwan) to prepare a 3% (g/mL) PLA solution in sample bottles. To ensure proper mixing, the solution was continuously stirred by a magnetic stirrer for 4 h. After mixing, the solution was cast on modified glass petri dishes and air-dried on a clean bench for 12 h. The modified glass petri dishes were purchased from the Duran Group (petri dish 23 755 39, STERIPLAN, Germany) and then modified dish depth to 3 mm by a glass workshop.

### Surface modification

**Plasma treatment.** Figure 1 shows the schematic diagram of the APP treatment system. The PLA films were treated in the post-discharge jet region of an atmospheric, nitrogen-based, parallel-plate ( $5 \times 5$  cm), dielectric barrier discharge (DBD). The film was placed on a moving stage to provide different residence times of treatment by controlling the number of passes and the moving speed (1–9 cm/s). The DBD system was driven by a 20–60 kHz quasi-pulsed power supply (EN Technologies model Genius 2). Both the dielectric layers (quartz) and the gap distance between them are kept at 1 mm throughout the study. In this study, two-step plasma treatment was carried out by two plasma treatments in sequence: (1) a pretreatment plasma treatment to pretreat the surface using the N<sub>2</sub> DBD jet with 0.1% addition of O<sub>2</sub> and a moving speed of 1 cm/s for 40 passes, and (2) an ammonia plasma treatment to incorporate amino functional groups using the same N<sub>2</sub> DBD jet, but with the addition of 5% NH<sub>3</sub> and a moving speed of 2 cm/s for 80

**TABLE I. Test Condition of Two-Step Plasma Treatment**

Two-Step Plasma Treatment		
Conditions	Pretreatment Plasma Treatment	Ammonia Plasma Treatment
Gas	N <sub>2</sub> + 0.1% O <sub>2</sub>	N <sub>2</sub> + 5% NH <sub>3</sub>
Flow rate	50 slm	10 slm
Gap distance	1 mm	
Dielectric	Quartz (1 mm)	
Input power	500 W	400 W
Frequency	60 kHz	30 kHz
Treatment distance	4 mm	
Moving speed	1 cm/s	2 cm/s
Number of treatment passes	40	80

passes. The equivalent exposure time was estimated to be 4 s for each step of the plasma treatment. The equivalent exposure time was used to estimate the total treatment time of plasma on the sample as the product of the gap distance and the number of treatment passes divided by the moving speed. Table I summarizes the details of the operating conditions of the pretreatment, ammonia, and two-step plasma treatments. In general, the total processing time ranged from 5 to 15 min for a complete two-step plasma treatment procedure if a PLA test surface with an area of  $4 \times 4 \text{ cm}^2$  was used.

**Gelatin coating treatment.** Gelatin powder from porcine skin (sigma, G1890-100G, type A) was dissolved in de-ionized water and stirred by a magnetic stirrer for 2 h to prepare a 0.1% (g/mL) gelatin solution. The solution was then poured through a  $0.22 \mu\text{m}$  filter (Nalgene) for sterilization. PLA films were then immersed in the sterilized gelatin solution for 1 h and air dried on a clean bench for 12 h. In general, the total treatment time ranged from 13 to 15 h using the gelatin coating method.

### Surface characterization

**Contact angle.** A contact angle machine (KRUSS GH100) was used to assess the surface wettability before and after plasma treatments. The static contact angle was measured using a de-ionized water droplet produced by a micropipette. The volume of the water droplet was kept at  $4 \mu\text{L}$ . An image of the water droplet was captured and imported into image analyzer software to evaluate the contact angle with Laplace-Young curve fitting. In addition, the contact angles presented in this study were obtained as average values by conducting the experiment at least three times.

**Calculation of surface energy.** The relationship between the surface energy (solid surface energy,  $\sigma_s$ ) and contact angle is formulated through Young's equation,  $\sigma_s = \gamma_{sl} + \sigma_l \cdot \cos\theta$ ,<sup>19</sup> where  $\sigma_s$  is the solid surface energy. Note  $\gamma_{sl}$  represents the interfacial energy between solid and liquid. The surface energy of the probe liquid is represented by  $\gamma_l$ , which was determined by experiments. The measured contact angle is denoted by  $\theta$ .

According to Owens-Wendt's method,<sup>20</sup> the surface energy of a solid ( $\sigma_s$ ) and a liquid ( $\sigma_l$ ) can be divided into two components, polar, and dispersion, as follows:  $\sigma_s = \sigma_s^p + \sigma_s^d$  and  $\sigma_l = \sigma_l^p + \sigma_l^d$ . Based on Wu's method,<sup>21</sup> combining the harmonic mean equation,<sup>6</sup>  $\gamma_{sl} = \sigma_s + \sigma_l - (\frac{4\sigma_l^p \cdot \sigma_s^p}{\sigma_l^p + \sigma_s^p} + \frac{4\sigma_l^d \cdot \sigma_s^d}{\sigma_l^d + \sigma_s^d})$ , and the equations mentioned above, the overall surface energy and individual polar and dispersive components can be readily derived. Both de-ionized water and diiodomethane (CH<sub>2</sub>I<sub>2</sub>) were used as the probe liquid. For de-ionized water,  $\sigma_l$ ,  $\sigma_l^p$ , and  $\sigma_l^d$  are 72.88, 50.4, and 21.6 mJ/m<sup>2</sup>, respectively. For di-iodomethane,  $\sigma_l$ ,  $\sigma_l^p$ , and  $\sigma_l^d$  are 50.00, 2.3, and 47.7 mJ/m<sup>2</sup>, respectively.

**Attenuated total reflectance-Fourier transform infrared spectroscopy.** To analyze the functional groups incorporated into the PLA surface, attenuated total reflectance-Fourier transform infrared spectroscopy (ATR-FTIR; BRUKER, TENSOR 27) with a Ge crystal was used. A background spectrum was measured in the wave number range of 4000–600 cm<sup>-1</sup> by keeping the resolution at 4 cm<sup>-1</sup> and the number of scans set at 32. After scanning the background signal, PLA film samples with and without plasma treatment were placed on the sample holder and scanned under the same conditions as the background scan. At least three measurements of each sample were taken to reduce the experimental uncertainties.

**X-ray photoelectron spectra (XPS).** The surface chemical composition before and after plasma treatments was measured by an X-ray photoelectron spectrometer (ESCA PHI 1600). The samples were measured using a Mg anode at 250 W and 15 KV, 1253.6 eV. In addition, the electron take-off angle with respect to the sample surface and the chamber pressure were kept at 45° and below  $2 \times 10^{-8}$  torr, respectively, during the measurement.

**Atomic force microscopy.** The Atomic force microscopy (AFM) images for measuring surface roughness were obtained by the Veeco Dimension 5000 Scanning Probe Microscope (D5000). This AFM consists of a micro-scale cantilever with a sharp tip (probe) at its end that is used to scan the specimen surface. When the probe scans very close to the sample surface, the interaction force between probe and sample can be measured by the deformation of cantilever, which is detected through a laser beam and a light detector. Tapping mode was adopted for the scan. The Z-axis information shows the roughness of the sample, and X-axis and Y-axis show the AFM scanning area. Three types of data can be acquired, including 2D and 3D morphology, step profile, and roughness analysis.

### Biological test

**Cell culture.** C<sub>2</sub>C<sub>12</sub>, mouse muscle myoblast cells (BCRC, 60083), were cultured in a T75 flask (BD, 353110) with Dulbecco's modified eagle's medium (DMEM, Gibco, 12800-017) supplemented with 10% fetal bovine serum (FBS, Biowest), penicillin-streptomycin (Gibco, 15140-122) and 1.5 g/L sodium bicarbonate (sigma, S5761). The cells were

cultured in an incubator (Heraeus, HELACELL 150) with 5% CO<sub>2</sub> at 37°C. While the cells grew into confluence, they were washed twice by Dulbecco's phosphate-buffered saline (DPBS, Gibco, 21600). Afterwards, trypsinization was used with 1 mL Trypsin-EDTA (sigma, T4174) for 1.5 min. Digestion was then blocked by the addition of 4 mL of culture medium. The culture medium was then piped back and forth to disperse the cells. The number of cells was counted using a hemacytometer (sigma, Z359629). Finally, cells ( $7 \times 10^4$  cells/mL) were seeded on a modified glass petri dish with pure, plasma treated, and gelatin-coated PLAs for later observation and tests.

**Inverted contrasting microscope.** Cell morphology is a good indicator for surface-cell compatibility. Cell morphology observations on pure, plasma treated and gelatin coated PLAs were performed using an inverted contrasting microscope (Leica, DM IL) during the 3-day period. These observations were performed at the 24, 48, and 72 h of treatment.

**MTT assay.** An MTT cytotoxicity test provides a measure of the integrity and activity of mitochondria in the cells, which may be linked to the viability and number of cells in a culture. The tetrazolium salt MTT is converted into a colored formazan product by mitochondria in healthy cells. Using dimethyl sulfoxide (DMSO) to release the colored product into solution, cell viability can be assessed by measuring the optical density (OD) of the solution. In this study, OD was assessed three times (at 24, 48, and 72 h) during the 3-day period for the pure, plasma treated, and gelatin coated PLAs. During the assay, the medium was replaced with 0.1 g/L MTT(sigma, M2128) in DMEM + 10% FBS, and the test samples were incubated for 4 h at 37°C with 5% CO<sub>2</sub>. After incubation, the formazan was dissolved using DMSO (sigma, D5879) and agitated with a pipette until no change of color was observed. The optical density of the fluid was then read at a wavelength of 570 nm by a microplate photometer (Thermo Scientific, Multiskan EX).

## RESULTS

### Results of surface characterization with and without plasma treatments

**Contact angle measurement.** Figure 2 shows the hydrophilic properties of the pure and plasma treated PLA surfaces obtained by contact angle measurements, which are performed immediately after the plasma treatment. For those applications which can only occur long after the treatment, more thorough aging test of the surface properties and corresponding biological tests are definitely required in the near future. The results show that the contact angle of pure PLA (0 passes) is approximately 73°. After pretreatment plasma treatment, the contact angle decreases to ~50° with the number of passes exceeding 10. The contact angle of ammonia plasma treatment decreases with an increasing number of passes and saturates at ~58° with pass counts beyond 80. For the two-step plasma treatment, two-step (40) performs generally better than two-step (10)

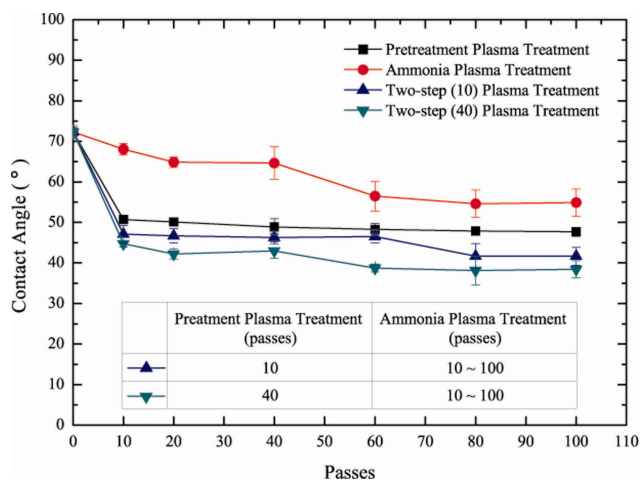


**FIGURE 2.** Contact angle measurements with and without different plasma treatments. [Color figure can be viewed in the online issue, which is available at [wileyonlinelibrary.com](http://wileyonlinelibrary.com).]

in terms of contact angle. Note the former and latter two-step plasma treatment represent that 40 and 10 passes of the plasma pretreatment were applied, respectively, with 80 passes of ammonia plasma treatment. The lowest contact angle found is ~38° using two-step (40); this is termed “two-step plasma treatment” as summarized in Table I, and as presented earlier. In short, by using a two-step plasma treatment, the PLA surface can be easily turned from hydrophobic to hydrophilic.

**Surface energy analysis.** Surface energy analysis was calculated using Wu's method as presented earlier. Figure 3 shows the calculated results of the surface energy for pure and plasma treated PLAs. The results show that the total solid surface energy and polar components of surface energy increase from 57.5 and 11 mJ/m<sup>2</sup> to 70.5 and 28 mJ/m<sup>2</sup>, respectively, using the two-step (40) plasma treatment. Interestingly and importantly, the large increase of the polar component may play an important role in enhancing the biocompatibility of PLA.

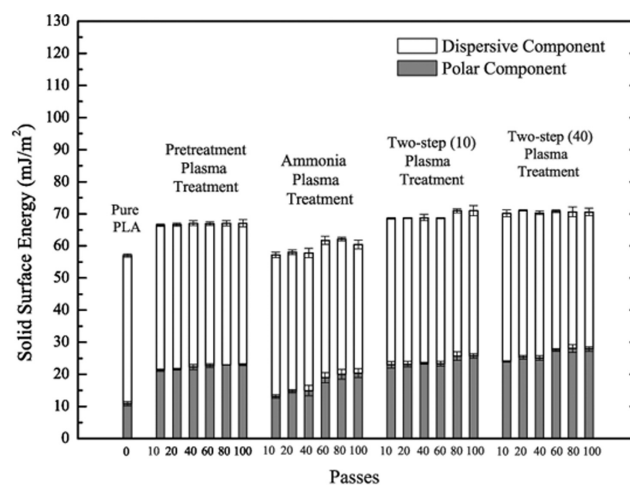


**FIGURE 3.** Surface energy analysis under pure and two-step plasma treated PLA surface.

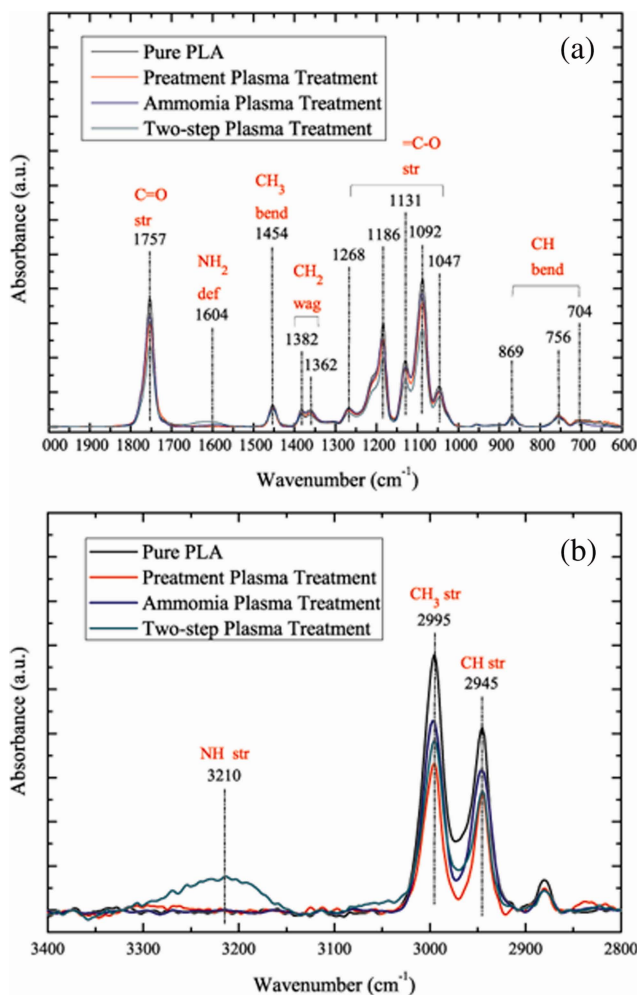


**FIGURE 4.** ATR-FTIR analysis of pure and plasma treated PLA surface (a) 600–2000  $\text{cm}^{-1}$ ; (b) 2800–3400  $\text{cm}^{-1}$  [Color figure can be viewed in the online issue, which is available at [wileyonlinelibrary.com](http://wileyonlinelibrary.com).]

**ATR-FTIR analysis.** ATR-FTIR analysis was utilized to identify the functional groups incorporated into the PLA surface after plasma treatments. Figure 4(a,b) shows that the absorbance intensity of primary amine<sup>22</sup>, including  $\text{NH}_2$  deformation ( $1604 \text{ cm}^{-1}$ ) and NH stretch ( $3210 \text{ cm}^{-1}$ ), increases, especially when using the two-step plasma treatment. It was reported that the plasma treatment changes surface properties within only a few nanometers<sup>23</sup> of the surface. In addition, the penetration depth of the ATR-FTIR into the sample is in the range of 200–1000 nm,<sup>24</sup> which is much larger than that of the plasma treatment. This finding means that the actual increase of the primary amine composition near the surface layer is much larger than those shown in Figure 4(a,b).

**XPS analysis.** The surface chemical compositions of the plasma treated and untreated PLAs were measured by an XPS analysis. Figure 5 shows that the PLA surface exhibits the highest N1s intensity using the two-step plasma treatment. Pretreatment and ammonia plasma treatment obtain nearly the same N1s intensity which is much lower than that of the two-step plasma treatment. To further understand the chemical

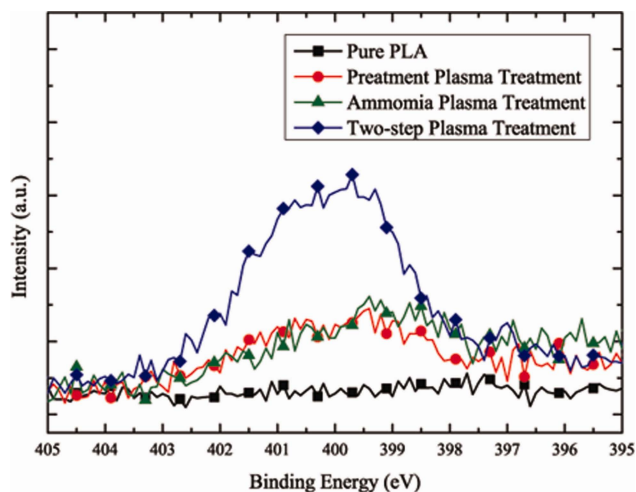


**FIGURE 5.** N1s intensity of pure and plasma treated PLA films. [Color figure can be viewed in the online issue, which is available at [wileyonlinelibrary.com](http://wileyonlinelibrary.com).]

bonding concentrations of each element, we de-convoluted the XPS spectra based on the analysis of the ATR-FTIR results.

Figure 6(a–c) shows the photoelectron spectra of C1s, O1s, and O1s on two-step plasma treated PLA surface. In addition, Table II summarizes the de-convoluted atomic concentrations. The C1s spectra are split up into C–C, C–H ( $285 \text{ eV}$ ), C–O ( $287 \text{ eV}$ ), C=O ( $289.2 \text{ eV}$ ),<sup>25</sup> and C– $\text{NH}_2$  ( $285.6 \text{ eV}$ )<sup>26</sup> with plasma treatments. Moreover, only C–N ( $400.1 \text{ eV}$ )<sup>27</sup> is used for the N1s spectra. The results show that the concentration of N/C ratio, which represents the amount of amine functional groups, can increase up to 19.1% with the proposed two-step plasma treatment to a value that is much larger than that of pure PLA and other treatments (approximately 4–6%). These results reveal that, by using a two-step plasma treatment, one can incorporate an appreciable amount of amine functional groups into the PLA surface in a very short period of time. In addition, the O/C ratio of the pretreated sample increases to 57% compared to that of the pure PLA sample ( $\sim 37\%$ ). Thus, the oxygen related functional groups are incorporated efficiently into the PLA surface. The oxygen related functional groups may also contribute to the highest N/C ratio using the two-step plasma treatment, which deserves further investigation to further understand the underlying mechanism.

**AFM analysis.** Figure 7 shows the results of the AFM analysis. The surface roughness (rms) of the original PLA is approximately 0.88 nm. After applying pretreatment, ammonia plasma treatment, and two-step plasma treatment, the roughness (rms) becomes 50.16, 1.50, and 73.22 nm, respectively. The pretreatment using  $\text{N}_2/\text{O}_2$  plasma contributes most to the roughness increase of the PLA surface up to 50 nm from 1 nm of the untreated PLA surface. The increase of roughness is mainly caused by the etching of oxygen radicals generated from the  $\text{N}_2/\text{O}_2$  plasma, which are carried downstream from the discharge region. Surprisingly and interestingly, the two-step plasma treatment

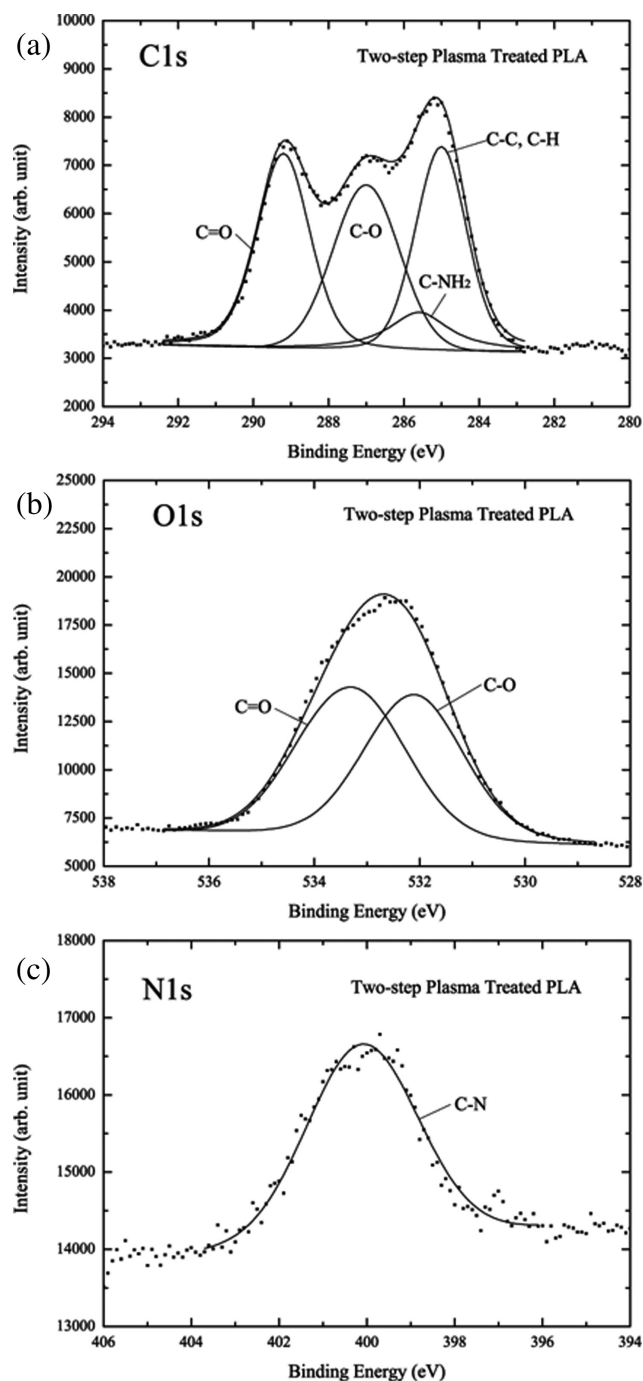


**FIGURE 6.** (a) C1s, (b) O1s and (c) N1s photoelectron spectrum of two-step plasma treated PLA surface.

further increases the surface roughness to approximately 72 nm, even though the second-step plasma treatment alone (ammonia plasma) shows essentially no influence on the surface roughness. The underlying physics of this observation requires further investigation.

**Results of biological tests using pure, two-step plasma treated, and gelatin coated PLAs**

**Cell morphology, attachment, and proliferation.** Figure 8 shows the cell morphology at different times using different

**TABLE II. Atomic Concentration and De-convoluted Information of Pure and Plasma Treated PLA Films Using XPS Analysis**

Conditions	Atomic Concentration		C1s Component			O1s Component		N1s Component		Atomic Ratio		
	C1s (%)	C-C and C-H (%)	C-O (%)	C=O (%)	C-NH <sub>2</sub> (%)	O1s (%)	C-O (%)	C=O (%)	N1s (%)	C-N (%)	N/C (%)	O/C (%)
Pure PLA	73	47.6	26.2	26.2	0	27	50	50	0	0	0	36.8
Pretreatment	61.2	35.1	29.2	29.9	5.8	34.9	49.6	50.4	3.9	100	6.3	57
Ammonia	68	42.9	26.1	26.9	4.1	29.1	49.6	50.4	2.9	100	4.2	42.8
Two-step	55.5	30.4	29.7	30.4	9.5	33.9	48.8	51.2	10.6	100	19.1	61

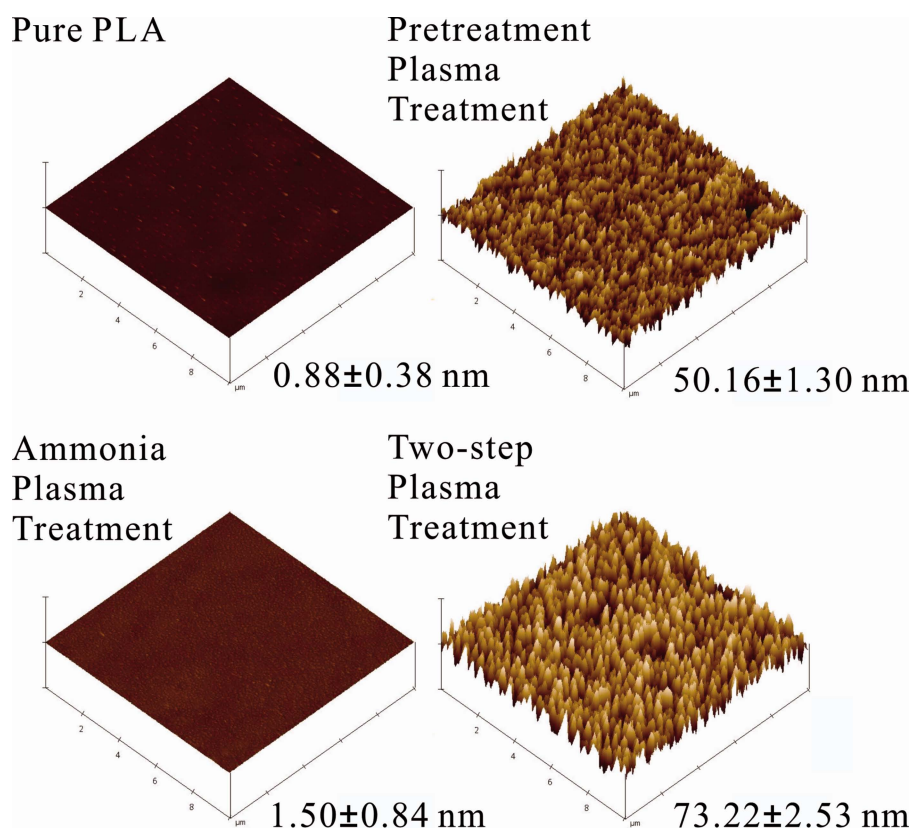


**FIGURE 7.** AFM analysis of pure and plasma treated PLA films. [Color figure can be viewed in the online issue, which is available at [wileyonlinelibrary.com](http://wileyonlinelibrary.com).]

plasma treatment procedures for the substrate preparation. Cell images on the pure PLA surface show a weakly adhered morphology. Moreover, the number of adhered cells is low after 24 h of culture. In contrast, the cell images on the two-step plasma treated surface exhibit a flattened morphology, and the attached number is much higher than that on pure PLA. After 48 h of culture, the two-step plasma treated PLA surface shows a higher proliferation ability compared to that of the pure PLA. The highest number of cells is found to attach on the two-step plasma treated PLA after 72 h of culture, which shows nearly full cell confluency, comparable with (or even better) than the confluency with the conventional gelatin coating method. In short, cell attachment and proliferation can be greatly enhanced by using the proposed two-step plasma treatment.

Figure 9 shows the number of cells and the activity of mitochondria assessed by the MTT assay. The cell attachment and proliferation tests show that the OD (optical density) using the two-step plasma treatment is approximately two times larger than when using the pure PLA sample (roughly the same as those by plasma pretreatment and ammonia treatment) and always slightly higher than when using the gelatin coating method after 72 h of culture; these findings are in agreement with visual observations in Figure 8, as mentioned earlier. Note that the magnitude of OD correlates with the number of healthy cells per unit area.

The results of the cell morphology observations are consistent with those of the MTT assay presented above. Thus,

we conclude that better cell attachment and proliferation using the two-step plasma treatment is obtained compared to when using the pure PLA without any treatment. In addition, the two-step plasma treatment can compete with and even perform better than the gelatin coating method in terms of its effectiveness in cell attachment and proliferation.

#### DISCUSSION

Figure 10 shows the sketches of the surface conditions of the pure, two-step plasma treated, and gelatin coated PLA films, when they are immersed in a culture medium, respectively. It is known that cells attach to a material surface only when either an adsorbed protein layer or ligands exist. Moreover, most proteins reveal hydrophobic features and favor attaching to a hydrophobic surface.<sup>28</sup> For the pure PLA case, few proteins from the culture medium may attach to the surface due to the hydrophobicity of PLA. These proteins may primarily contribute to the modest observed cell attachment and proliferation on the pure PLA surface. However, the effectiveness of these proteins alone is insufficient to compete with that of the two-step plasma treatment and the gelatin coating method, according to the biological results described earlier.

In the gelatin coating case, abundant amino acids and hydrolyzed collagen are coated on the PLA surface. These can be regarded as contributing a great quantity of cell binding sites on the surface, which results in greatly

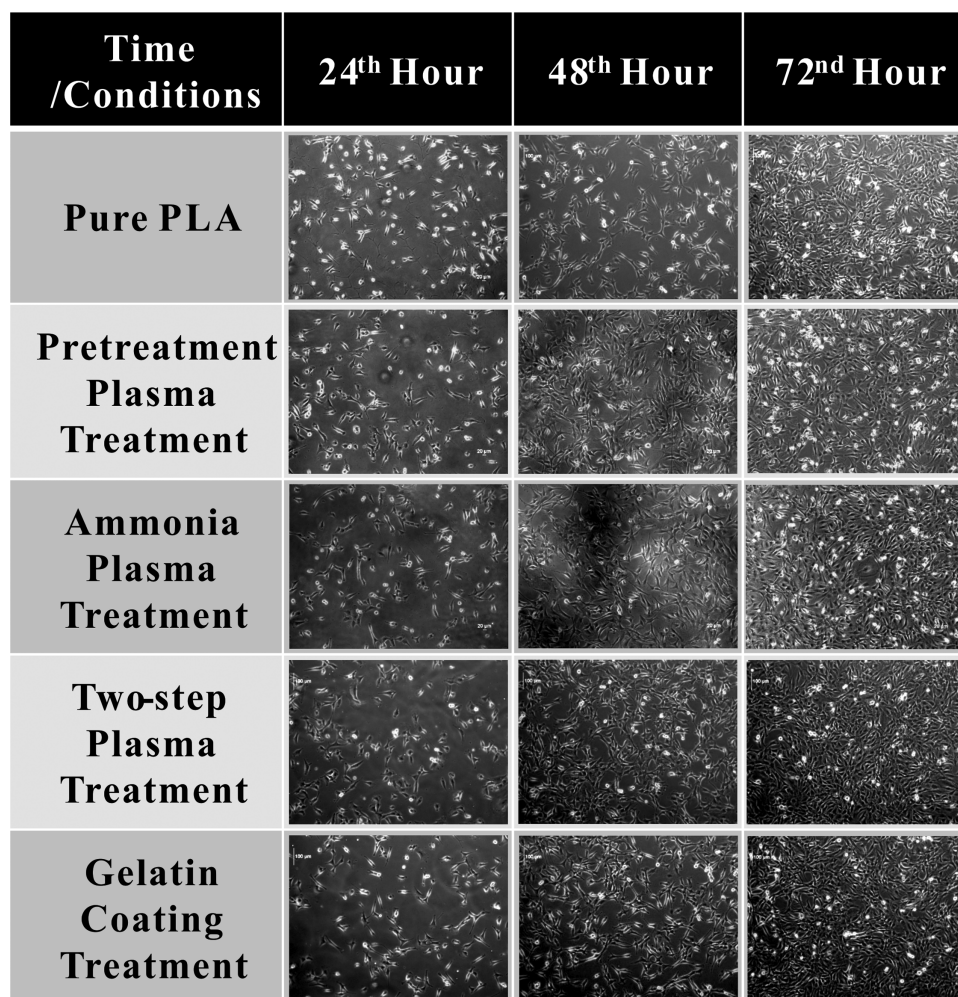


**FIGURE 8.** Inverted contrasting microscope observation of cells on pure, gelatin coated and 2-step plasma treated PLA films during three-day test period.

improved cell attachment and proliferation in which the OD is about two times higher than that of pure PLA after 72 h of culture.

The PLA surface using the two-step plasma treatment exhibits the highest surface energy, especially in the polar component, and thus an enhanced hydrophilic property. The resulting surface energy and contact angle are approximately  $70.5 \text{ mJ/m}^2$  and  $38^\circ$ , respectively. Most proteins are difficult to attach to a hydrophilic surface.<sup>28</sup> Thus, the effect of proteins absorbed on the two-step plasma treated PLA surface can be neglected. The most critical contribution to the enhanced cell attachment and proliferation should be the high amount of amine functional groups, which can covalently couple with the ligands from the culture medium,<sup>15,29</sup> as well as other modified surface properties, such as surface roughness and surface energy. Note that the cell membrane is a phospholipid bilayer in which the outer polar head, which directly contacts the environment, exhibits hydrophilic characteristics.<sup>30</sup> In other words, cells exhibit high affinity to a hydrophilic surface. After cells contact with the surface, the integrins on the cell membrane can further react with the ligands bonded on the amine func-

tional groups and transduce signals for the cells to attach and proliferate on the surface. In addition, cells prefer to adhere to surfaces with a high surface energy,<sup>31</sup> especially with a high polar component,<sup>32</sup> and to migrate on rougher

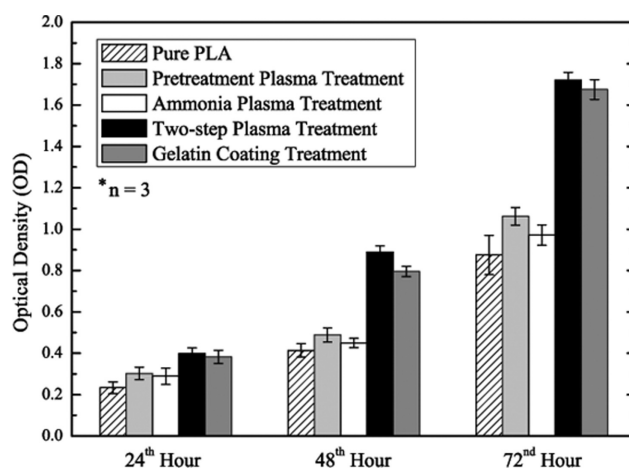


**FIGURE 9.** Optical Density (OD) of cells on pure, gelatin coated and 2-step plasma treated PLA films for a three-day test period.





**FIGURE 10.** Sketches of the surface conditions of pure, two-step plasma treated and gelatin coated PLA films with immersed in culture medium. [Color figure can be viewed in the online issue, which is available at [wileyonlinelibrary.com](http://wileyonlinelibrary.com).]

surfaces,<sup>30</sup> which is beneficial to cell proliferation. The surface chemical and physical properties obtained by the two-step plasma treatment on a PLA surface are all in favor of cell attachment and proliferation, as we have observed in this study. These properties may explain the reasons that the two-step plasma treatment performed as well or even better than the gelatin coating method in terms of cell attachment and proliferation effectiveness.

The comparison of the preparation duration between the two-step plasma treatment and the gelatin coating treatment is discussed next. The plasma exposure time of the former treatment is only 8 s, but the realistic preparation time includes setting up and removing samples on a moving stage as well as other necessary operations. It is worth noting that these procedures are all indispensable. Therefore, the two-step plasma treatment takes about 5–15 min. On the other hand, the latter treatment takes at least 13–15 h. Obviously, the preparation for the proposed two-step plasma treatment is much faster than that of the gelatin coating treatment. This finding implies that the proposed two-step APP treatment can meet some of the criteria of tissue engineering for practical applications.

## CONCLUSION

In this article, a two-step plasma treatment procedure using the post-discharge jet region of a parallel-plate, nitrogen-based DBD is proposed and investigated experimentally. Using the two-step plasma treatment, we can effectively and efficiently incorporate primary amine groups into the PLA surface. The results show that N/C ratio can reach 19.1% on the PLA surface. Furthermore, after applying the two-step plasma treatment, the surface energy, contact angle, and surface roughness are improved to 70.5 mJ/m<sup>2</sup>, 38°, and 73.22 nm, respectively. These modified surface properties are confirmed to be very beneficial in improving cell attachment and proliferation on the PLA surface for mouse muscle myoblast cells (C<sub>2</sub>C<sub>12</sub>). In comparison with the conventional gelatin coating method, the proposed two-step plasma treatment procedure can produce a PLA surface with almost the same (or even better) cell attachment and cell proliferation for muscle cells, while requiring a reduced preparation time (5–15 min vs. 13–15 h). In summary, the

proposed two-step plasma treatment procedure under atmospheric conditions can not only promote cell attachment and proliferation but also dramatically speed up the substrate preparation time. This represents a potential method for making tissue engineering more practical. Several issues remain unsolved in this study, and thus deserve future investigation, including a detailed mechanism of the incorporation of functional groups and applicability of the method to other types of polymers, different types of cells and even three-dimensional scaffolds.

## ACKNOWLEDGMENTS

The authors also thank Prof. T.-K. Wu of NCTU for kindly providing the microplate photometer (Thermo Scientific, Multiskan EX).

## REFERENCES

- Ikada Y. Challenges in tissue engineering. *J R Soc Interface* 2006; 3:589–601.
- Lanza RP, Langer R, Vacanti J. *Principles of Tissue Engineering*, 2nd ed. Boston: Elsevier; 2007.
- Barrera DA, Zylstra E, Lansbury PT, Langer R. Synthesis and RGD peptide modification of a new biodegradable copolymer: poly (lactic acid-co-lysine). *J Am Chem Soc* 1993;115:11010–11011.
- Gupta AP, Kumar V. New emerging trends in synthetic biodegradable polymers—Polylactide: A critique. *Eur Polym J* 2007;43: 4053–4074.
- Anselme K. Osteoblast adhesion on biomaterials. *Biomaterials* 2000;21:667–681.
- Yildirim ED, Ayan H, Vasilets VN, Fridman A, Gucer S, Friedman G, Sun W. Effect of dielectric barrier discharge plasma on the attachment and proliferation of osteoblasts cultured over poly( $\epsilon$ -caprolactone) scaffolds. *Plasma Process Polym* 2007;4:58–66.
- Humphries JD, Byron A, Humphries MJ. Integrin ligands at a glance. *J Cell Sci* 2006;119:3901–3903.
- Chu CR, Coutts RD, Yoshioka M, Harwood FL, Monosov AZ, Amiel D. Articular cartilage repair using allogeneic perichondrocyte-seeded biodegradable porous polylactic acid (PLA): A tissue-engineering study. *Biomed Mater Res* 1995;29:1147–1154.
- Jiao YP, Cui FZ. Surface modification of polyester biomaterials for tissue engineering. *Biomed Mater* 2007;24:R24–R37.
- Hou X, Zhang BL, She F, Cui YL, Shi KY, Yao KD. Surface of gelatin modified poly(L-lactic acid) film. *Chinese J Polym Sci* 2003;21: 227–283.
- Kazuaki N, Takeo M. Observation of cell shortening and dynamic changes of actin filaments during cell detachment from thermoresponsive-gelatin-coated substrate. *JSME Int J Ser C Mech Syst* 2005;48:411–418.

12. Soradech S, Nunthanid J, Limmatvapirat S, Luangtana-anan M. An approach for the enhancement of the mechanical properties and film coating efficiency of shellac by the formation of composite films based on shellac and gelatin. *J Food Eng* 2012;108:94–102.
13. Kostov KG, dos Santos ALR, Honda RY, Nascente PAP, Kayama ME, Algatti MA, Mota RP. Treatment of PET and PU polymers by atmospheric pressure plasma generated in dielectric barrier discharge in air. *Surf Coat Tech* 2010; 204:3064–3068.
14. Steen ML, Hymas L, Havey ED, Capps NE, Castner DG, Fisher ER. Low temperature plasma treatment of asymmetric polysulfone membranes for permanent hydrophilic surface modification. *J Membr Sci* 2001;188:97–114.
15. Hutmacher DW, Schantz T, Zein I, Ng KW, Teoh SH, Tan KC. Mechanical properties and cell cultural response of polycaprolactone scaffolds designed and fabricated via fused deposition modeling. *J Biomed Mater Res* 2001;55:203–216.
16. Webb K, Hlady V, Tresco PA. Relative importance of surface wettability and charged functional groups on NIH 3T3 fibroblast attachment, spreading, and cytoskeletal organization. *J Biomed Mater Res* 1998;41:422–430.
17. Mortensen H, Kusano Y, Leipold F, Rozlosnik N, Kingshott P, Goutianos S, Sørensen BF, Stenum B, Bindslev H. Modification of glassy carbon surfaces by atmospheric pressure cold plasma torch. *Jpn J Appl Phys* 2006;45:8506–8511.
18. Klages CP, Grishin A. Plasma amination of low-density polyethylene by DBD afterglows at atmospheric plasma. *Plasma Process Polym* 2008;5:368–376.
19. Tadmor R. Line energy and the relation between advancing, receding, and Young contact angles. *Abs Pap Am Chem* 2004;20:7659–7664.
20. Owens DK, Wendt RC. Estimation of the surface free energy of polymers. *J Appl Polym Sci* 1969;13:1741–1747.
21. Wu S. Polar and nonpolar interactions in adhesion. *J Adhes* 1973; 5:39–55.
22. Socrates G. *Infrared and Raman characteristic group frequencies*, 3rd ed. New York: Wiley; 2001.
23. Tang CY, Kwon YN, Leckie JO. Probing the nano- and micro-scales of reverse osmosis membranes—A comprehensive characterization of physiochemical properties of uncoated and coated membranes by XPS, TEM, ATR-FTIR, and streaming potential measurements. *J Membr Sci* 2007;287:146–156.
24. Kwon OJ, Tang S, Myung SW, L N, Choi HS. Surface characteristics of polypropylene film treated by an atmospheric pressure plasma. *Surf Coat Tech* 2005;192:1–10.
25. Vincent Crist B. *Handbook of Monochromatic XPS Spectra: Semiconductors*. New York: Wiley; 2000.
26. Everhart DS, Reilley CN. Chemical derivatization in electron spectroscopy for chemical analysis of surface functional groups introduced on low-density polyethylene film. *Abs Pap Am Chem S* 1981;53:665–676.
27. Lahaye J, Nanse G, Bagreev A, Strelko V. Porous structure and surface chemistry of nitrogen containing carbons from polymers. *Carbon* 1999;37:585–590.
28. Lampin M, Warocquier-Clerout R, Legris C, Degrange M, Sigot-Luizard MF. Correlation between substratum roughness and wettability, cell adhesion and cell migration. *J Biomed Mater Res* 1996;36:99–108.
29. Quirk RA, Davies MC, Tendler SJB, Shakeshefi KM. Surface engineering of poly(lactic acid) by entrapment of modifying species. *Macromolecules* 2000;33:258–260.
30. Nagle JF, Tristram-Nagle S. Structure of lipid bilayers. *Biochem Biophys Acta* 2000;1469:159–195.
31. Schakenraad JM, Busscher HJ, Wildevuur CRH, Arends J. The influence of substratum surface free energy on growth and spreading of human fibroblasts in the presence and absence of serum proteins. *J Biomed Mater Res* 1986;20:773–784.
32. Comelles J, Estévez M, Martínez E, Samitier J. The role of surface energy of technical polymers in serum protein adsorption and MG-63 cells adhesion. *Nanomedicine Nanotechnol* 2010;6:44–51.